Nuclear Instruments and Methods in Physics Research A 766 (2014) 221–224

Contents lists available at ScienceDirect

Nuclear Instruments and Methods in Physics Research A

journal homepage: www.elsevier.com/locate/nima

Determination of tolerances of mirror displacement and radiator gas impurity for the CBM RICH detector

J. Adamczewski-Musch [a], K.-H. Becker [b], S. Belogurov [c], N. Boldyreva [d], A. Chernogorov [c], C. Deveaux [e], V. Dobyrn [d], M. Dürr [e], J. Eom [f], J. Eschke [a], C. Höhne [e], K.-H. Kampert [b], V. Kleipa [a], L. Kochenda [d], B. Kolb [a], J. Kopfer [b], P. Kravtsov [d], S. Lebedev [e], E. Lebedeva [e], E. Leonova [d], S. Linev [a], T. Mahmoud [e,*], J. Michel [a], N. Miftakhov [d], Y. Nam [f], W. Niebur [a], K. Oh [f], E. Ovcharenko [c], C. Pauly [b], J. Pouryamout [b], S. Querchfeld [b], J. Rautenberg [b], S. Reinecke [b], Y. Riabov [d], E. Roshchin [d], V. Samsonov [d], J. Song [f], O. Tarasenkova [d], T. Torres de Heidenreich [a], M. Traxler [a], C. Ugur [a], E. Vznuzdaev [d], M. Vznuzdaev [d], J. Yi [f], I.-K. Yoo [f]

[a] GSI Darmstadt, Germany
[b] University Wuppertal, Germany
[c] ITEP Moscow, Russia
[d] PNPI Gatchina, Russia
[e] University Gießen, Germany
[f] Pusan National University, Republic of Korea

ARTICLE INFO

Available online 6 May 2014

Keywords:
CBM RICH detector
Mirror displacement
Gas contamination

ABSTRACT

The CBM experiment at the future FAIR facility will explore nuclear matter at high net-baryon densities. One of the key observables is di-leptons as they penetrate the created matter without further strong interactions. A gaseous RICH detector in a standard projective geometry using spherical mirrors is one of two detector elements for the required electron identification. The mirror system consists of about 72 trapezoidal mirror tiles. Any misalignment between the tiles relative to the nominal common spherical surface leads to reduction of the reconstruction efficiency of Cherenkov rings and deterioration of their resolution. To determine tolerances in mirror misalignment extensive simulation and measurement studies were carried out. Pure CO_2 will be used as radiator gas. Gas contamination, mainly moisture and Oxygen, reduces the number of detected photons per ring and worsens the quality of reconstructed Cherenkov rings. Therefore a study was carried out to determine tolerances in radiator gas contamination.

1. Introduction

The Compressed Baryonic Matter (CBM) experiment is a dedicated heavy-ion experiment at the future FAIR facility in Darmstadt. It will explore the intermediate range of the QCD phase diagram through several physical signatures. Two important ones are low-mass vector mesons and charmonium, which are accessible through their di-leptonic decay channel. In CBM, electrons with momenta below 8 GeV/*c* will be mainly identified with a Ring Imaging Cherenkov detector (RICH) [1].

The concept of the RICH detector foresees a 1.7 m long CO_2-radiator, a plane of spherical mirror tiles, and multianode photomultiplier tubes (MAPMTs) as photon detectors. The mirror tiles are made of glass with a reflective $Al+MgF_2$ coating [2]. The approx. 72 mirror tiles have a trapezoidal shape of about $40\times40\ cm^2$ with a curvature radius of 3 m and a thickness of 6 mm. To provide stable supply of pure CO_2 to the radiator volume a gas system was constructed, which keeps the detector volume under an overpressure of 2 mbar relative to the atmospheric pressure. The gas flow is controlled via a slow control system to stabilize the internal detector pressure by adding more or less fresh pure gas. A purifier and a dryer are part of the system to remove moisture and Oxygen from the recirculation flow.

2. RICH prototype

To verify the detector concept and to evaluate the combined performance of the three main components (gas, mirror, and

* Corresponding author.
E-mail address: Tariq.Mahmoud@exp2.physik.uni-giessen.de (T. Mahmoud).

http://dx.doi.org/10.1016/j.nima.2014.04.074
0168-9002/

MAPMT) a laterally scaled prototype has been constructed. The mirror system consists of four real-dimension mirror tiles. Each tile is mounted to a common aluminum frame at three points and can be displaced at those points via remotely operated actuators (Fig. 1 left). The photon detector system consists of several MAPMTs and Multichannel Microchannel Plates (MCP-PMTs). This prototype was tested in two testbeam campaigns in fall 2011 and 2012 at the CERN PS T9 facility [3]. In order to evaluate its performance the prototype was implemented in the CbmROOT simulation framework. Systematic studies of a large variety of performance parameters have been done among which were the radiator gas purity (gas system performance) and the adjustment of the mirror tiles aiming at determination of acceptable tolerances.

The right panel of Fig. 1 shows a typical example of a measured electron ring. Simulations and measurements show a number of hits per electron ring of $n_{hits} \approx 24$ at atmospheric pressure and room temperature. Rings are reconstructed and fitted with a circle and an ellipse. On average the ring radius is 44.54 mm and the major axis of the ellipse-fit (called A-axis) is 43.36 mm indicating a slight ellipticity in the shape of the Cherenkov ring. The minor to major axis ratio is about 0.945.

3. Tolerances in mirror displacement

When constructing the mirror plane, misalignment between the tiles relative to the nominal common spherical surface is

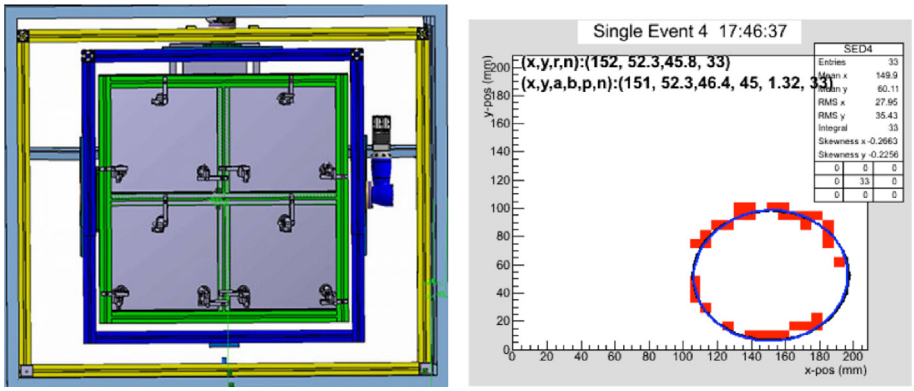

Fig. 1. Left: system of mirror tiles in the CBM-RICH prototype. Right: Cherenkov ring from a typical single 3 GeV/c-electron with a circle fit.

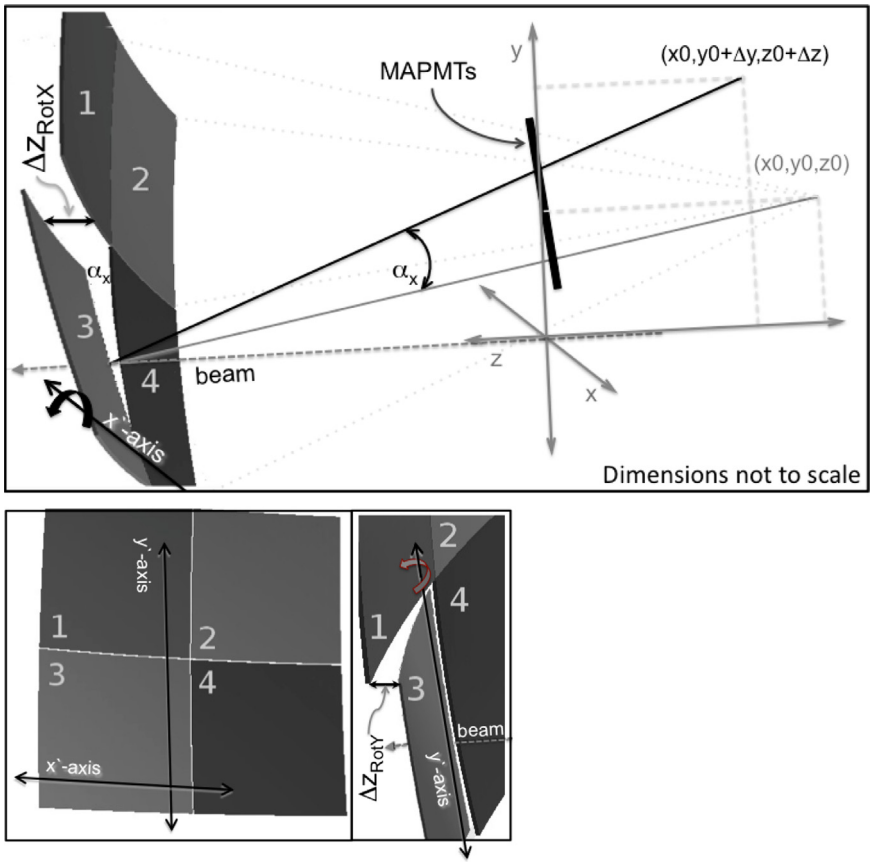

Fig. 2. Up: displacement of the top side at mirror number 3, Δz_{RotX}. The black (grey) solid line connects the beam position on the mirror surface with the middle point of the sphere before (after) the rotation. Bottom left: the $x'-y'-$plane on the mirror surface. Bottom right: Δz_{RotY} displacement.

unavoidable. This can displace the hit position of reflected photons on the detector plane as illustrated in Fig. 2. Consequently the resolution and efficiency of reconstructed Cherenkov rings suffer. To determine displacement tolerances this aspect was simulated and addressed during the beam time. In the experiment misalignment is induced by the three actuator structure in the prototype. Data have been taken with electrons at a momentum of 3 GeV/c. The beam center runs exactly between mirrors number 3 and number 4. In this study the main focus is on the A-axis.

The upper side of mirror number 3 was displaced backwards and the left side forwards, see Fig. 2. These displacements are called Δz_{RotX} and Δz_{RotY} respectively. Δz_{RotX} corresponds to a rotation around the $x'-$axis by an angle α_X and Δz_{RotY} corresponds to a rotation around the $y'-$axis by an angle α_Y.

3.1. Rotation around $x'-$axis

Fig. 3 shows the A-axis distributions as a function of Δz_{RotX}. Starting from the ideal case with $\Delta z_{RotX}=0$, the mean value and the FWHM of the A-axis distribution grow with Δz_{RotX}. The first falls again at a displacement of $\Delta z_{RotX}=1.3$ mm and the later grows up to a value of about FWHM=9 mm.

The displacement (rotation) causes the half ring, which is reflected on the rotated mirror (# 3) to move along the photon detector plane upwards and the two separated half rings thus starts forming an ellipse. For small displacements the ring finder still finds one "ring" and the ring fitter fits it but with a larger A-axis. The larger the displacement the larger is the splitting of both halves and consequently the A-axis grows more and more leading to higher mean values. At $\Delta z_{RotX}\approx 1.3$ mm the splitting is pronounced enough such that the ring finder recognizes two rings, compare the left panel of Fig. 4. Then, both semi-rings can be fitted with more realistic values of the A-axis. This partial regeneration of the ring shape is misleading because two rings instead of one are recognized. Each of the semi-rings has an n_{hits} of approximately half as much as in the ideal case. This worsens the fit quality and widens the distribution (larger FWHM). Notice that for $\Delta z_{RotX}>1.3$ mm the hits are concentrated at one side of the fitted rings. This is why FWHM does not regenerate at high displacements as does the mean value.

The right panel of Fig. 4 shows measured distributions of the A-axis for several Δz_{RotX}. The results agree with the simulations qualitatively and we can state that displacements can be tolerated as long as they are lower than $\Delta z_{RotX}=0.32$ mm corresponding to a rotation of $\alpha_X\approx 1$ mrad.

3.2. Rotation around $y'-$axis

The same study as discussed before has been done for rotations around the $y'-$axis, see Fig. 4 right and Fig. 5. With increasing Δz_{RotY} the mean value of the A-axis distributions decreases and its width increases. The rotation moves one half of the ring towards the other; as seen in the right panel of Fig. 4, the ring is squeezed leading to lower values of the A-axis and subsequently to the reduction of the mean value. The growth in the distribution width is due to the lower n_{hits} attached to the squeezed ring.

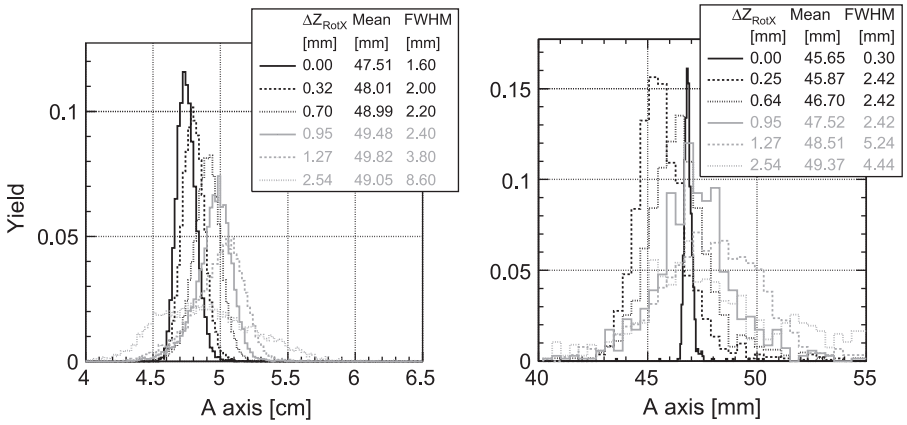

Fig. 3. A-axis distributions for several Δz_{RotX} displacements. Left: simulations. Right: measured data.

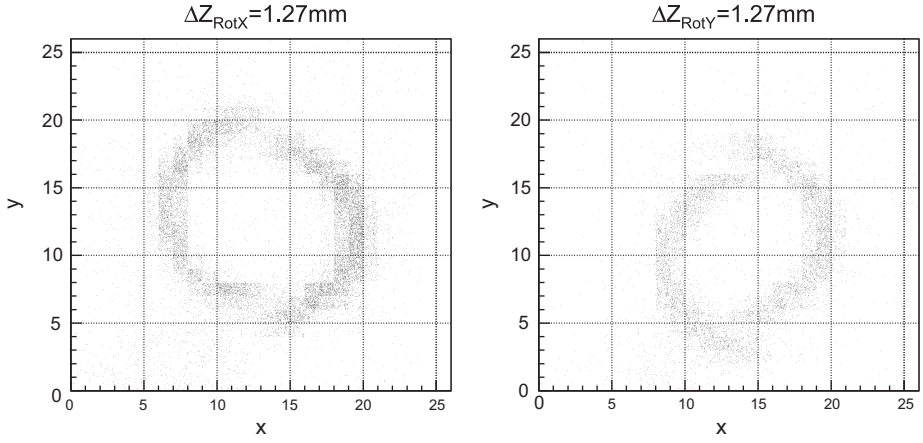

Fig. 4. Measured integrated rings for a Δz_{RotX} (left) and Δz_{RotY} (right) displacement of 1.27 mm each. The up-down asymmetry in the right panel is due to an additional Δz_{RotX} displacement.

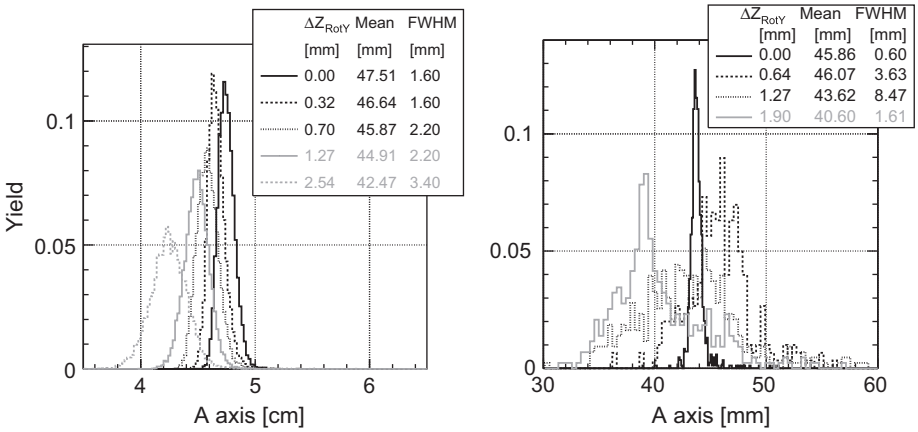

Fig. 5. *A*-axis distributions for several Δz_{RotY} displacements. Left: simulations. Right: measured data.

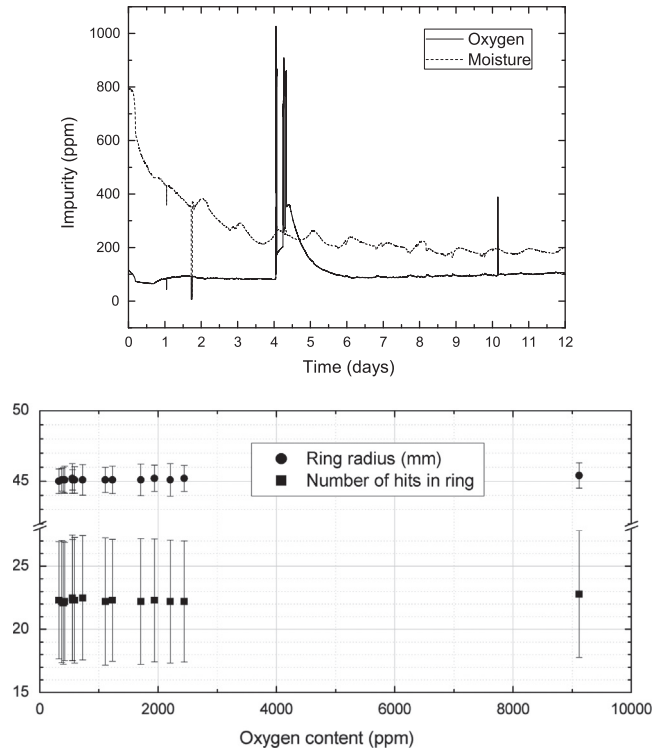

Fig. 6. Upper panel: oxygen and moisture content in the radiator gas during the beam time. Lower panel: ring radius and number of hits per ring in dependence on the oxygen content in the radiator gas.

As before, results from data and simulation agree qualitatively and indicate that a displacement of $\Delta z_{RotY} = 0.32$ mm ($\alpha_Y \leq 1$ mrad) is tolerable.

3.3. Other displacements

The discussed results take only Δz_{RotX} backwards and Δz_{RotY} forwards into account. Δz_{RotX} forwards has same effects as backwards due to symmetry reasons. Δz_{RotY} backwards has an opposite effect as Δz_{RotY} forwards: instead of being squeezed, the ring is stretched causing a wider distribution of the *A*-axis. The two ring halves separate quickly at Δz_{RotY} of about 0.4 mm and the ring finder recognizes two rings. This keeps our conclusions regarding tolerances unchanged.

4. Tolerances of gas impurity

During both beam periods the gas system worked very stable and could keep the RICH gas box under the anticipated overpressure of 2 mbar relative to the atmospheric pressure. As for the gas contamination, mainly oxygen and moisture, the system works sufficiently well and reduces them down to 100 ppm and 200 ppm respectively as seen in the upper panel of Fig. 6. To determine contamination tolerances the radiator gas was artificially contaminated with air. The measured Oxygen (moisture) level has been increased to 1% (1100 ppm). Even this high contamination does not affect the measured number of photons per ring and the ring radius, see the lower panel of Fig. 6.

5. Conclusion

To achieve electron identification up to $p=8$ GeV/c in the CBM experiment, a RICH concept has been established with three main components: CO_2 as radiator gas, spherical glass mirrors, and MAPMTs as photon detector. The RICH concept could successfully be confirmed by intensive and detailed studies including simulations and measurements with a laterally scaled prototype.

Tolerances on mirror displacements of up to 0.32 mm at any mirror side were determined from beamtime data in comparison to simulations. Gas impurities of up to 1% oxygen content do not harm the number of hits per ring.

Acknowledgments

This work was supported by the Hessian LOEWE initiative through the Helmholtz International Center for FAIR, by the GSI F&E-Cooperation with Gießen and Wuppertal (WKAMPE1012), by BMBF Grants 05P12RGFCG, 05P12PXFCE and 05P09PXFC5, by the National Research Foundation of Korea (2012004024), and by Helmholtz Grant IK-RU-002 and SC ROSATOM through FRRC.

References

[1] B. Friman, et al., (Eds.), The CBM Physics Book, Lecture Notes in Physics, vol. 814, Springer-Verlag, Berlin, Heidelberg, 2011.
[2] C. Höhne, et al., Nuclear Instruments and Methods in Physics Research Section A 639 (2011) 294.
[3] J. Adamczewski-Musch, et al., Nuclear Instruments and Methods in Physics Research A (2014), these proceedings.